17th World Conference on Earthquake Engineering, 17WCEE
Sendai, Japan - September 13th to 18th 2020

OBSERVATIONAL FRAGILITY MODELS FOR MASONRY BULDINGS USING DAMAGE DATA FROM THE 2012 EMILIA EARTHQUAKES

E. Simoni[(1)], N. Buratti[(2)], C. Mazzotti[(3)], A.B. Costantino[(4)]

[(1)] *Assistant researcher, DICAM - University of Bologna, elena.simoni8@unibo.it*
[(2)] *Associate professor, DICAM - University of Bologna, nicola.buratti@unibo.it*
[(3)] *Professor, DICAM - University of Bologna, claudio.mazzotti@unibo.it*
[(4)] *Emilia-Romagna Regional Agency for Territorial Safety and Civil Protection, Antonio.Costantino@regione.emilia-romagna.it*

Abstract

Seismic fragility models are important elements for risk prediction, loss-estimation and emergency planning, because they define the relationship between different damage levels and the intensity of ground-shaking. These models can be obtained using different methods, among which the most common are (*i*) nonlinear numerical simulations and (*ii*) statistical analysis of observational damage data. The present paper presents seismic fragility models for masonry structures, derived using the second approach on damage data collected after the 2012 earthquake that struck northern Italy. These data were obtained from rapid post-earthquake evaluation-forms issued by the Italian Civil Protection Department, which are compiled after seismic events by qualified engineers for assessing damage in buildings. The damage reported in these documents was converted to a five-level scale derived from the European Macroseismic Scale EMS-98. Since data in the rapid evaluation forms may be incomplete with reference to undamaged buildings, their number was estimated considering also census data. A total of about 60000 masonry buildings were analyzed. In order to define fragility models, damage data must be combined with the ground-shaking intensity at the location of each building. To this aim, various ground-motion intensity measures among those proposed in the literature (e.g. PGA, spectral accelerations, Housner spectrum intensity), were considered. Specific ground-motion attenuation relationships and spatial correlation models were calibrated for all the intensity measures taken into account, using data from the strongest earthquakes of the 2012 Emilia seismic sequence. Shake maps were then computed using a multivariate log-normal approximation for the ground-motion intensity spatial distribution. Finally, a probit generalized linear model was employed in order to fit parametric fragility models. The paper discusses the fragility models obtained and analyzes the correlation among different ground-motion intensity measures ad damage.

Keywords: seismic fragility; observational damage data; masonry buildings.

1. Introduction

Earthquakes are still a relevant cause of human and economic losses; therefore, it is important to have reliable tools to predict damage scenarios and risk, in order to properly plan civil protections strategies and to guide political choices aimed at reducing risk and losses. The availability of fragility models for specific building typologies and thus the knowledge of which areas of a city or region is more likely to report severe damage, can be fundamental in the organization of a timely and efficient risk and emergency management.

Fragility is here intended as the probability of exceeding a certain level of damage in a given building class conditioned on ground-motion intensity. It can be expressed either in discrete form, through Damage Probability Matrices (DPMs) or by means of parametric or non-parametric curves. DPMs were first defined by Whitman [1] in 1973. Their first application to European buildings was proposed by Braga et al. [2] and was based on damage data of Italian buildings after the 1980 Irpinia earthquake. Spence at al. [3] provided an example on how to derive fragility functions using survey data on a worldwide scale and used the Parameterless Scale of Intensity PSI to measure ground-motion intensity. This approach was later adopted by Orsini [4], which limited the range of the analysis to damage data from the 1980 Irpinia earthquake. Post-earthquake surveys from the 2002 Molise earthquake were used by Goretti and Di Pasquale [5] to relate the observed damage distribution to the seismic intensity and to different building types. A larger database of post-earthquake surveys from several Italian events was used by Rota et al. [6] to first obtain DPMs and then derive fragility curves through nonlinear regression. Eleftheriadou and Karabinis [7] as well, addressed seismic fragility by means of DPMs based on post-earthquake surveys carried out after the 1999 Athens earthquake.

Due to its still relatively recent occurrence, there are only very limited works where fragility models were calibrated using data from the 2012 Emilia earthquakes in Italy. Models have been proposed mainly for RC precast industrial buildings [8], which represented the most damaged building class from these events [9]. Fragilities for masonry and reinforced concrete buildings of this region have been studied by Ioannou et al. [10] and Verderame et al. [11], respectively.

This work makes use of three ground-motion Intensity Measures (IMs) in order to derive parametric fragility curves for masonry buildings using data form the 2012 Emilia earthquakes. Shake maps for the provinces of Modena, Bologna and Ferrara, were computed through specifically defined attenuation relationships, while damage data was obtained from post-earthquake survey forms. The paper discusses the fragility models obtained and analyzes the correlation among different ground-motion intensity measures and damage.

2. The 2012 Emilia earthquakes

The 2012 Emilia earthquakes consisted of a seismic sequence of moderate intensity events, which occurred near the province of Modena, in northern Italy, and affected neighbouring cities such as Bologna and Ferrara. The strongest shocks struck on 20th and 29th May and had moment magnitudes of 6.1 and 6.0, respectively [12]. In that area events with comparable magnitude were not recorded in recent times, even though there is historical evidence of similar occurrences around 1340 and 1570 near Ferrara and in 1570 and at the beginning of the XX century in the area of Finale Emilia (Modena) [13]. Damage produced by the 2012 earthquakes was mainly due to the lack of seismic design for the buildings in the area, which was not classified as seismic until 2003.

In the following, only events with $M_w \geq 5$ and with information about the geometry of the rupture plane were considered, for a total of four events. Earthquake and ground-motion data was obtained from the ITACA database [10]. Fig. 1 shows the location of the epicentres of the considered events and the surface projection of the associated rupture planes.

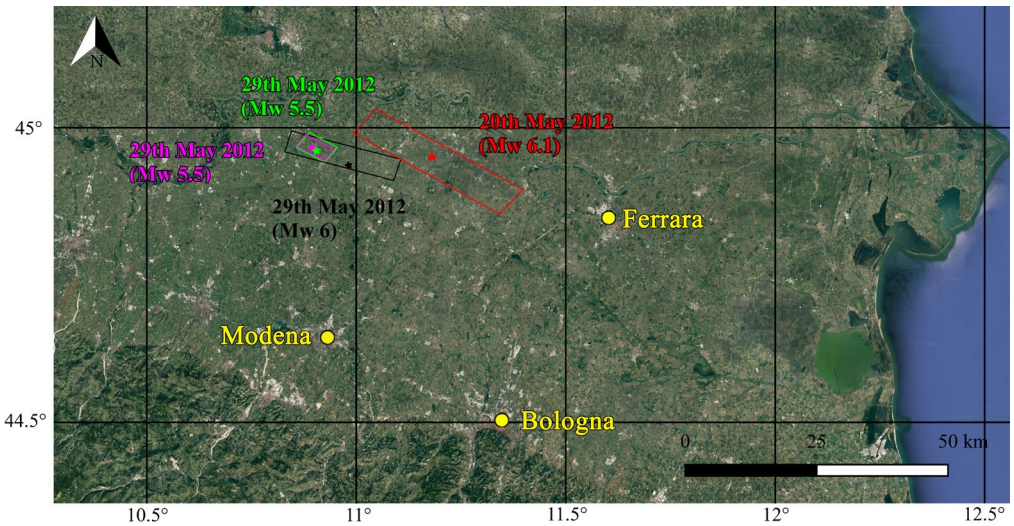

Fig. 1 - Finite faults models for the four considered seismic events.

3. Seismic action characterization

In order to define fragility models, it is necessary to combine data about ground-motion intensity and damage. Three IMs were chosen to measure the level of ground-shaking: i) Peak Ground Acceleration (PGA), which is traditionally used in the definition seismic hazard maps [6] and often adopted in fragility models, even though Rossetto and Elnashai [14] have shown that it does not always correlate well with observed damage; ii) Housner's Spectral Intensity (SI_H) which is correlated to hysteretic energy demand on structures and is computed from spectral velocity [15]; iii) the mean spectral pseudo-acceleration between T = 0.1 s and T = 0.5 s (PSA_{0105}). This range of periods was adopted because the majority of masonry buildings in the area under investigation have no more than two storeys. In order to estimate IM values in the area of interest, shake maps were computed, as described in the following.

3.1 Ground motion attenuation

To evaluate IMs levels at locations far from ground motion recording stations, shake maps are needed. In the present work, given the large number of accelerograms recorded, it was chosen to develop specific Ground Motion Prediction Equations (GMPEs) to compute shake maps, rather than adopting GMPEs from the literature. To this aim, values for all the considered IMs were calculated in the MATLAB [16] environment for all the recordings of the horizontal components of ground-motions recorded by accelerometric stations at epicentral distances shorter than 200 km [10]. The number of ground motion recording stations associated with each considered event is shown in Table 1 along with the event moment magnitude.

Table 1 – number of recording stations for each considered seismic event.

No.	Date	Mw	Number of stations
1	20th May	6.1	120
2	29th May	6	123
3	29th May	5.5	141
4	29th May	5.5	37

Furthermore, as suggested by Boore et al. [17], directivity was considered by combining the orthogonally oriented components of horizontal ground shaking provided by each recording station, in order to define an orientation independent intensity. Then the median value of the intensity was considered to obtain the measures GMRotD50 [17], i.e. the 50th percentile of the geometric mean, taken over all nonredundant rotations between 0 and 90 degrees. Introducing directivity in the derivation of GMPEs allows to refine the seismic source description in the predictive relations and not fall into an oversimplified formulation. The functional form adopted for the GMPEs for all the studied IMs is the following:

$$\ln(IM_{ij}) = c_1 + c_2 \cdot M_{ij} + c_3 \cdot \ln\left(\sqrt{R_{ij}^{\ 2} + c_4^{\ 2}}\right) + f_{site,ij} + \delta_{b,j} + \delta_{w,ij}, \tag{1}$$

where IM_{ij}, is the IM value at the *i*-th recording station of the *j*-th earthquake, M_{ij} is the moment magnitude and R_{ij} is the Joyner-Boore distance in km, defined as the minimum horizontal distance of a point of interest to the surface projection of the rupture plane [18], $f_{site,ij}$ represents site effects, and $\delta_{b,j}$ and $\delta_{w,ij}$ are between- and within-event random factors, respectively. The lack of nonlinear magnitude terms in Eq.1 is justified by the limited range of moment magnitude values for the earthquakes under consideration, which varies from 5.5 to 6.1. The site effect term relies on the soil classification defined by Eurocode 8 [19], which is based on shear wave velocity values in the uppermost 30 m. The following expression is then adopted for the site effects term:

$$f_{site} = c_5 \cdot S_B + c_6 \cdot S_C + c_7 \cdot S_D \tag{2}$$

where

- $S_B = S_C = S_D = 0$ for soil type A ($V_{s,30} > 800$ m/s).
- $S_B = 1$, $S_C = S_D = 0$ for soil type B (360 m/s $< V_{s,30} \leq 800$ m/s).
- $S_C = 1$, $S_B = S_D = 0$ for soil type C (180 m/s $< V_{s,30} \leq 360$ m/s).
- $S_D = 1$, $S_B = S_C = 0$ for soil type D ($V_{s,30} < 180$ m/s).

This model could be implemented because the information regarding the soil type associated with each recording station was available in the adopted database. Regressions were performed for the three different IMs using the formulas shown in Eq. (1) and Eq. (2) by means of nonlinear mixed effects models in the R environment [20]. Fig. 2 shows the resulting attenuation for PGA alongside the ground motion recordings for the main 29th May event.

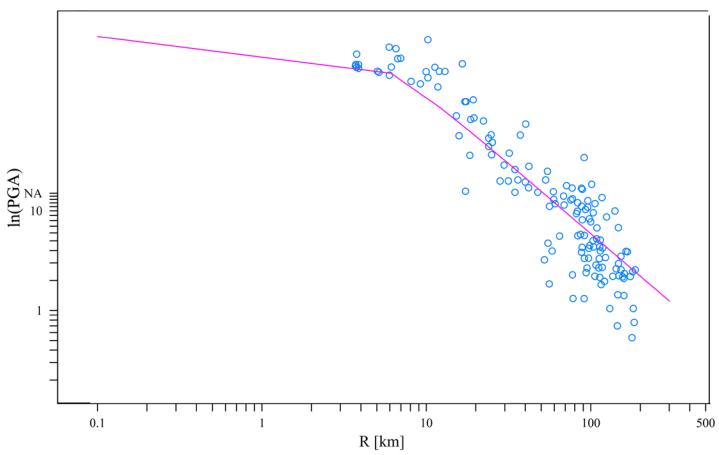

Fig. 2- Attenuation relationship for PGA. Blue dots represent the ground motion recordings from the main 29th May event.

3.2 Spatial correlation

As discussed by Baker et al. [14, 15], formulating shake maps requires the interpolation of IMs values over a spatial region, where their distribution is conditioned on observations at the arbitrary locations of ground-motion recording stations. Therefore, such joint predictions are possible only if a spatial correlation model is defined. The conditional distribution of the IM at a specific site, where no strong motion station exists, will differ from the unconditional distribution, which is provided by the GMPE [23], because of the non-zero value of the inter-event residual and the spatial correlation of the intra-event residual. Bradley [23] also observed that for cases where the site of interest is located far away from any strong motion station, the conditional distribution will be similar to the unconditional one, while for sites located very close to a strong motion station, the conditional mean will approach the value observed at the strong motion station.

In this work, a spatial correlation model was derived empirically by constructing semi-variograms for events with a sufficient number of ground motion recordings, namely the main event for the 29th May, using residuals from the regressions carried out to fit the GMPEs. Then a spherical semi-variogram model was fitted to the sample semi-variograms. This model is expressed as shown in Eq. (3)

$$\gamma(h) = \begin{cases} \dfrac{3h}{2a} - \dfrac{1}{2}\left(\dfrac{h}{a}\right)^3 & \text{for } 0 \le h \le a \\ 1 & \text{for } h > a \end{cases} \tag{3}$$

being a the range and h the separation distance. Below, Fig. 3 shows the fitted semi-variogram for PGA for the main event of the 29th May.

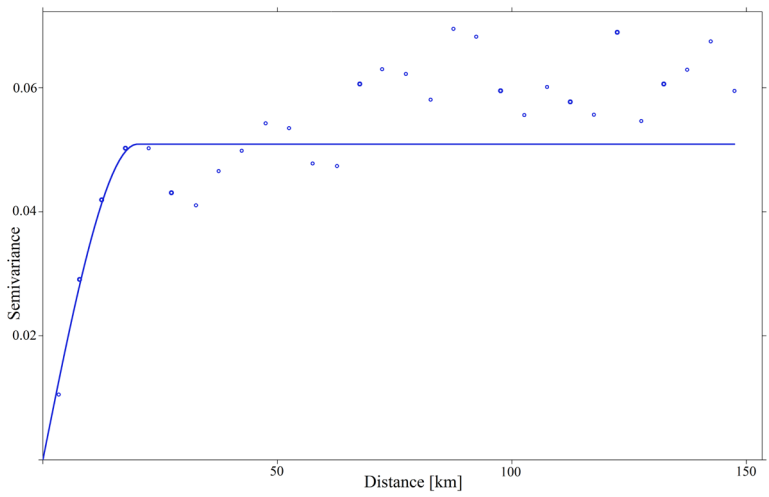

Fig. 3 - PGA semi-variogram for the main event of the 29th May 2012.

4. Shake maps for the main events of 20th and 29th May 2012

Shake maps rely on GMPEs to estimate the ground motion intensity over a spatial grid and then correct this distribution so that the estimated intensity in correspondence of recording stations coincides with the recorded value. It is thus assumed that the IM value associated with the recording stations has no uncertainty, while at every other location, the uncertainty related to the estimate depends on the distance from recording stations.

Shake maps are obtained following the procedure illustrated by Bradley [23–25] with the difference that the unconditional distribution derived from GMPEs is assumed to be equal to

$$\ln(IM_{es}) \sim N(\overline{\ln(IM_{es})}, \sigma_W{}^2) \tag{4}$$

The variance in Eq. (4) corresponds to the within-event variance only, because shake maps are here derived only for one seismic event at time. A regular grid with a spacing of 0.05° of latitude and longitude was used to construct the shake map that covers a square area centered on the epicentre of the chosen event, including portions of the Emilia-Romagna, Lombardy and Veneto regions. Information on the type of soil at all the grid points was not known, however, considering the geology of the area, soil type C was assumed for all the sites. As an example, Figs. 4 and 5 show the shake maps and the variance spatial distribution for PGA and PSA_{0105}.

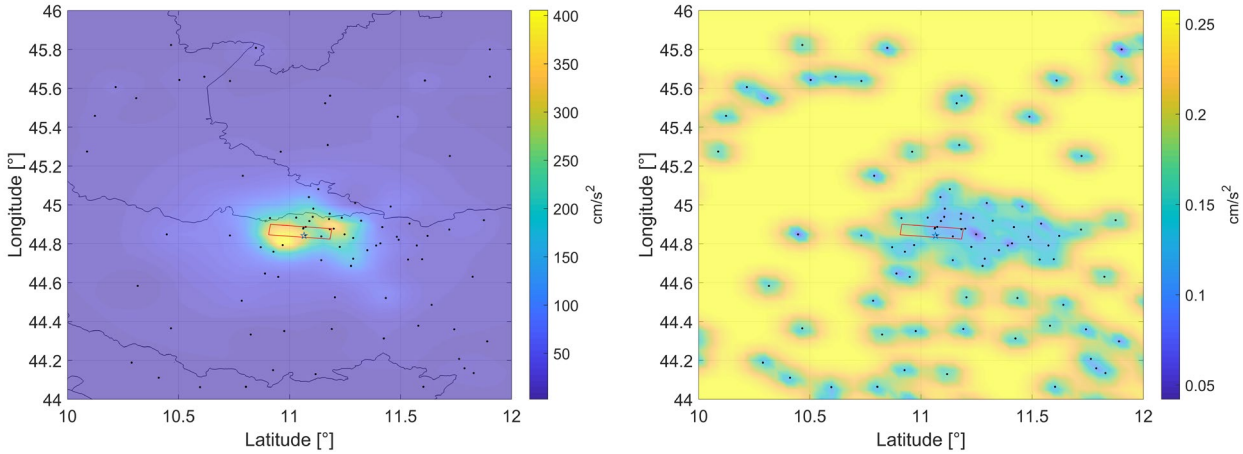

Fig. 4 - Median (left) and variance (right) shake maps for PGA for the main event of 29th May 2012. Black dots indicate ground-motion recording stations.

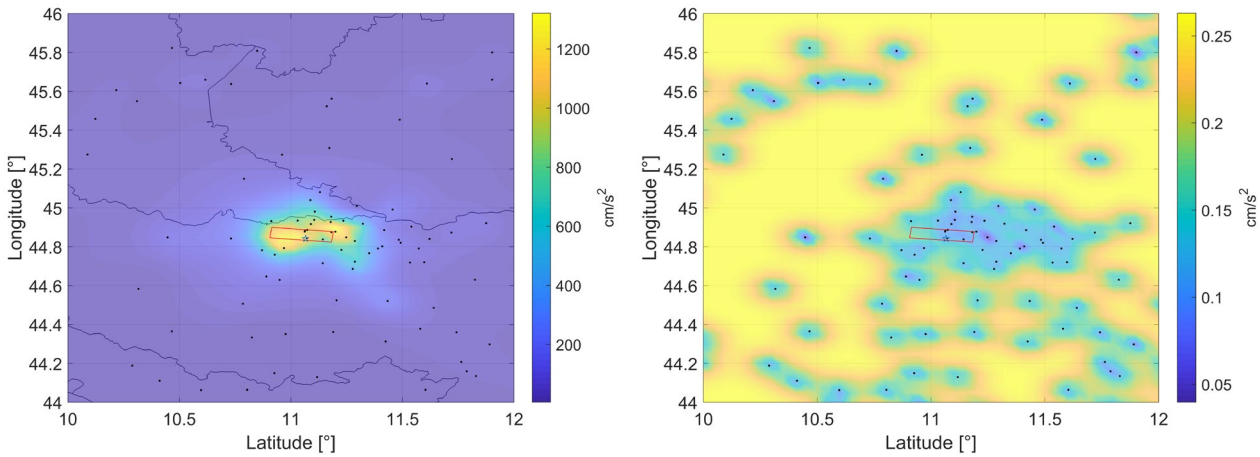

Fig. 5 - Median (left) and variance (right) shake maps for PSA_{0105} for the main event of 29th May 2012. Black dots indicate ground-motion recording stations.

5. Damage and building databases

Damage data was obtained from the *Da.D.O.* platform that stores the results of Italian post-earthquake surveys, specifically referred to as AeDES forms [26]. This type of form was introduced for the first time in

1997 after the earthquake that affected both the Umbria and Marche regions and was later updated after the earthquakes of Pollino in 1998 and Molise in 2002. It was also used in 2009 in Abruzzo and in 2012 in Emilia-Romagna. The AeDES forms allow to identify univocally each surveyed building and collect information regarding general features (e.g. the destination of use, dimensions, year of construction, retrofit interventions and occupancy), structural characteristics that can affect the seismic performance of buildings, location (vertical structures, slabs, stairs, roof, infills) and level of damage for structural components. A section referred to the detection of damage in non-structural components is also present. Masonry buildings can be distinguished based on materials, bond pattern, quality and type of masonry but also on the presence of tie-rods and on the stiffness of slabs.

Damage classification in these forms relies on nine sub-levels grouped in three macro-levels (D1, D2-D3, D4-D5) and is based on the Europeans Macroseismic Scale 1998, EMS-98 [27] and it was converted into a discrete five-level scale adopting the procedure proposed by Rota et al. [6]. Table 2 shows the scheme used to do so.

Table 2 - Conversion table of the AeDES forms damage levels to five damage states (adopted from Rota et al. [6]).

Damage state	**Description**	**AeDES form damage class**
D_0	No damage	Null
D_1	Light damage	Light (<1/3, 1/3 -2/3, >2/3)
D_2	Significant damage	Medium-severe (<1/3)
D_3	Severe damage	Medium-severe (1/3 - 2/3, >2/3)
D_4	Very severe	Very severe (<1/3, 1/3 – 2/3)
D_5	Partial collapse, collapse	Very severe (>2/3)

Post-earthquake surveys were compiled after the 20th May earthquake, but due to the occurrence of a second event on 29th May, they did not cover the whole number of damaged buildings. Therefore, they were compiled again after this second earthquake. Excluding areas with very-high levels of damage, post-earthquake surveys were performed on-demand and, for this reason, did not include the whole building population of the considered provinces of Bologna, Modena and Ferrara. However, these surveys were mandatory in order to access public funds for post-earthquake reconstruction, thus it is reasonable to assume that the vast majority of damaged buildings were assessed. Nevertheless, another database was required to obtain the total number of buildings. To this aim the data from the 2011 census compiled by the Italian National Institute of Statistics (ISTAT) was adopted, assuming that all the buildings not surveyed with the AeDES forms were undamaged.

The Da.D.O. platform provides around 22000 survey forms relative to the 2012 Emilia earthquakes, though, by comparison with literature works that derive empirical fragility curves using damage data from the same events [10], these seem to represent about the 50% of the complete damage database. Here we assume that these data are a representative sample of the full set of damaged buildings. Since the number of undamaged buildings introduced in the fragility assessment must be proportional to the available damage population, the census final count was halved in order to not underestimate fragility. It is duly noted that the results presented in the next paragraphs are not final and that they will be updated once the full damage database is available to the authors.

An important difference between the two data sources is that AeDES forms provided by Da.D.O. assign to each entry a set of coordinates in latitude-longitude format that define univocally the building or the aggregate. This information is not available in the 2011 census, where the location of the building is defined

only through ID codes (region, province, municipality) and address. A software developed for the Emilia-Romagna region was used to overcome this issue. Furthermore, a homogenisation procedure had to be carried out to merge the two databases. Mixed and reinforced masonry was removed, which is referred to as "other" in the census database. Non-identified structures were discarded from both databases, as well as RC frames, industrial and abandoned buildings. Entries from both databases that were not located in the provinces of Bologna, Modena and Ferrara were discarded. Municipalities without any post-earthquake survey were removed from the census database. As the main objective of the census is to provide information used in demography analyses, it does not contain many relevant data on structural typology. Thus, using census data imposed some limitations on the building class definition. Finally, it was also necessary to identify buildings that were surveyed by means of the AeDES forms and remove them from the census so that they would not be double counted in the fragility evaluation. After merging the two databases a total of 58842 buildings was obtained. Fig. 6 shows how these buildings and the associated damage level were distributed over the region.

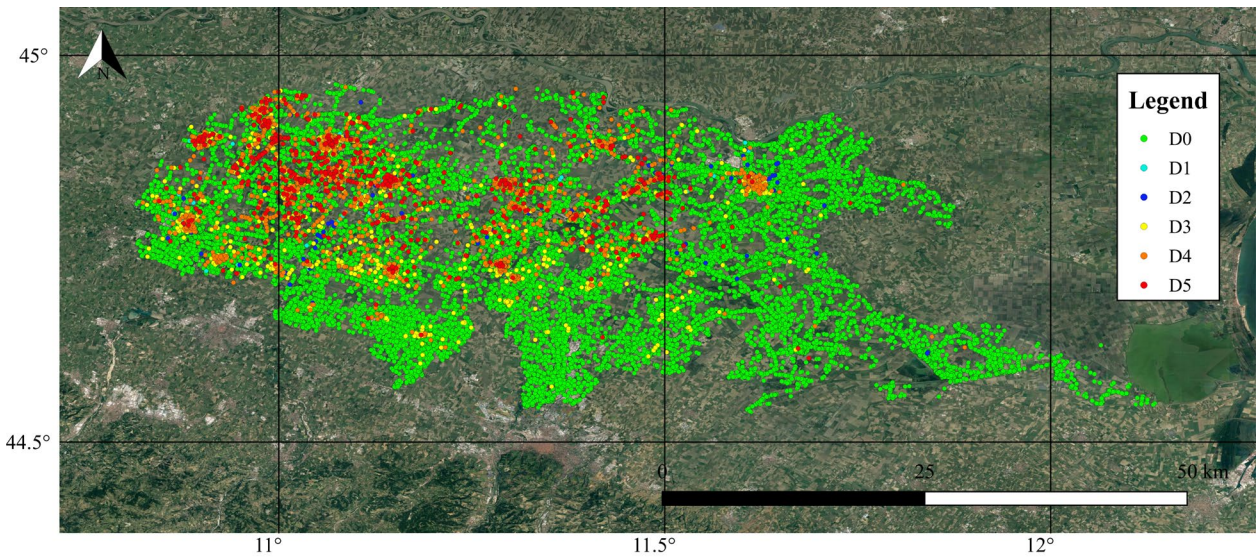

Fig. 6 – Building and associated damage distribution.

6. Fragility assessment

This section presents estimates of fragility models parametric curves. The ground motion intensity and damage data available are were used to fit parametric fragility functions in the form of generalised linear models [8]. A probit model was used express the exceedance probability for the damage state D_j, $p_{i,j}$, as a function of the ground-motion intensity IM.

$$\Phi^{-1}(p_j) = \beta_{0,j} + \beta_{1,j} \log_{10}(IM) . \tag{6}$$

In Eq. (6) Φ^{-1} indicates the inverse of the standard normal CDF and $\beta_{0,j}$, $\beta_{1,j}$ are unknown regression parameters. The logarithm of the ground motion intensity was considered as covariate to avoid non-zero damage probability when IM has zero value. The likelihood function L_j for the damage level D_j, is written according to Eq. (7).

$$L_j = P(y_j \mid \beta_{0j}, \beta_{1j}) = \prod_{i=1}^{N} (1 - p_{i,j}(IM_i; \beta_{0j}, \beta_{1j}))^{(1-y_{i,j})} p_{i,j}(IM_i; \beta_{0j}, \beta_{1j})^{y_{i,j}} \tag{7}$$

The probability $p_{i,j}$ is computed according to Eq. (6). In Eq. (7) $y_{i,j}$ is a binary variable that is equal to 1 if the damage D_i for the i-th building is equal or greater than D_j; it corresponds to 0 otherwise. The IM for the i-th building is defined as the maximum between the one related to the 20th May event and the one from the 29th event. Table 4 reports the estimates of the regression coefficients obtained by maximizing the likelihood function.

Analysis of deviance, intended as a generalization of the residual sum of squares, can be implemented to compare two or more models and was used in this work to find which of the considered IM can better relate to the observed damage. Deviance values for each damage level for PGA, PSA_{0105} and SI_H are presented in Table 5. Lower values of deviance were obtained with PSA_{0105} and this leads to thinking that this IM is better correlated with the observed damage and could be used in the definition of damage scenarios in case of future seismic events. Fig. 7 and Fig. 8 show the fragility curves obtained Eq.(6) and Eq. (7) and the estimates of the regression coefficients reported in Table 4.

Table 3 – Estimates of the regression coefficients for all damage states and for the considered IMs.

	β_0	β_1	β_0	β_1	β_0	β_1	β_0	β_1	β_0	β_1
IM	$D \geq D_1$		$D \geq D_2$		$D \geq D_3$		$D \geq D_4$		$D = D_5$	
PGA	-5.275	2.017	-5.188	1.962	-4.932	1.812	-5.593	1.897	-5.623	1.538
PSA_{0105}	-6.748	2.226	-6.586	2.153	-6.392	2.047	-6.950	2.078	-7.211	1.849
SI_H	-4.625	2.166	-4.546	2.101	-4.378	1.960	-4.777	1.927	-5.172	1.663

Table 4 - Deviance values obtained for three considered IMs.

IM	$D \geq D_1$	$D \geq D_2$	$D \geq D_3$	$D \geq D_4$	$D = D_5$
PGA	104208.74	102662.01	98981.24	70103.44	21985.02
PSA_{0105}	100696.78	99537.17	95669.53	68485.68	21422.09
SI_H	101924.96	100618.09	97055.04	69382.52	21609.51

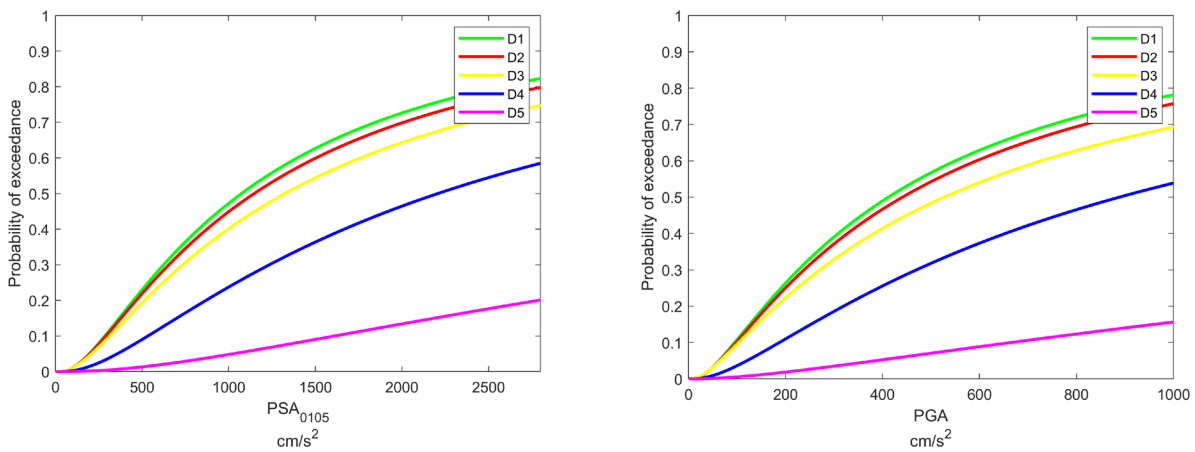

Fig. 7 – Fragility curves in terms of PGA (left) and PSA_{0105} (right) for all damage levels. Points represent the estimated exceedance probability value for each interval of Table 3.

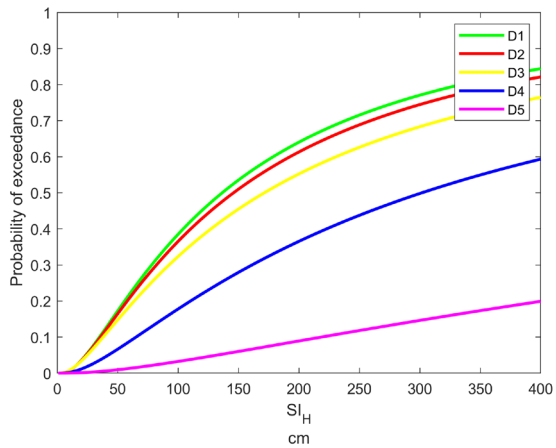

Fig. 8 - Fragility curves in terms of SI_H for all damage levels. Points represent the estimated exceedance probability value for each interval of Table 3.

From Fig.7 and Fig. 8 it can be seen that it is not possible to clearly distinguish damage levels 1 to 3. Since the AeDES survey forms were compiled mainly on-demand it is possible that buildings with light damage were not surveyed. Furthermore, the estimated probabilities of exceeding damage state D_5 are very low and, therefore, is not possible to have reliable evaluation of the fragility curve for high values ground-motion intensity.

7. Conclusions

This paper presented fragility models for masonry buildings, calibrated using damage data from the 2012 Emilia earthquakes. A damage database, containing around 60000 buildings, was created by combining information from the Da.D.O. database, that relies on the AeDES post-earthquake forms, and census data. A homogenisation procedure was also carried out so that elements from both data sources could be joined. Ground-motion recordings from four earthquakes with $M_w \geq 5$ were processed to compute values for three different ground motion intensity measures, which were then used to fit GMPEs and spatial correlation models. These models were then employed to compute shake maps that allowed to estimate the ground-motion intensity at the locations of all the buildings in the database.

Parametric fragility models were fitted first using a probit generalized linear model. Due to the features of the available damage data the resulting curves tend to estimate moderate exceedance probabilities, still consistent with empirical models in the literature. At the same time, it is also recognised that using a low-quality database, such as the 2011 Census, may have led to an overestimation of the undamaged building population, and, consequently, to an underestimation of fragility. The adopted methodology used to derive fragility curves may be further improved, assessing fragility with the whole damage database from the 2012 Emilia earthquakes, including the influence of uncertainty associated with the estimated IM values and considering the effect of consecutive events with similar intensity.

8. Acknowledgments

The authors would like to acknowledge the financial and technical support of the Emilia-Romagna Regional Agency for Territorial Safety and Civil Protection. The Statistics Service and Geographical Informative Systems of the Emilia-Romagna Region is also acknowledged for providing the software used to geocode census data.

9. References

[1] Whitman R (1973):Damage probability matrices for prototype buildings. .

[2] Braga F, Dolce M, Liberatore D (1982): A statistical study on damaged buildings and an esuing review of the MSK-76 scale.*7th European Conference on Earthquake Engineering*. .

[3] Spence R, Coburn AW, Pomonis A, Sakai S (1992): Correlation of ground motion with building damage: The definition of a new damage-based seismic intensity scale.*10th World Conference on Earthquake Engineering*. , 551–556.

[4] Orsini G (1999): A model for Buildings' Vulnerability Assessment Using the Parameterless Scale of Seismic Intensity (PSI).*Earthquake Spectra*. **15** (3), 463–483.

[5] Goretti A, Di Pasquale G (2004): Building inspection and damage data for the 2002 Molise, Italy, earthquake.*Earthquake Spectra*. **20** (SPEC. 1), 167–190.

[6] Rota M, Penna A, Strobbia CL (2008): Processing Italian damage data to derive typological fragility curves.*Soil Dynamics and Earthquake Engineering*. **28** , 933–947.

[7] Eleftheriadou AK, Karabinis AI (2008): Damage probability matrices derived from earthquake statistical data.*14th World Conference on Earthquake Engineering*. .

[8] Buratti N, Minghini F, Ongaretto E, Savoia M, Tullini N (2017): Empirical seismic fragility for the precast RC industrial buildings damaged by the 2012 Emilia (Italy) earthquakes.*Earthquake Engineering and Structural Dynamics*. **46** , 2317–2335.

[9] Savoia M, Buratti N, Vincenzi L (2017): Damage and collapses in industrial precast buildings after the 2012 Emilia earthquake.*Engineering Structures*. **137** , 162–180.

[10] Ioannou I, Verucci E, Arcidiacono V, Rossetto T (2018):Empirical Fragility Assessment of the Italian Masonry Buildings Using Data From the Emilia 2012. in: 16th Eur. Conf. Earthq. Eng., pp. 1–11.

[11] Verderame GM, Ricci P, De Luca F, Del Gaudio C, De Risi MT (2014): Damage scenarios for RC buildings during the 2012 Emilia (Italy) earthquake.*Soil Dynamics and Earthquake Engineering*. **66** , 385–400.

[12] Luzi L, Pacor F, Puglia R (2019): Italian Accelerometric Archive v3.0. Istituto Nazionale di Geofisica e Vulcanologia, Dipartimento della Protezione Civile Nazionale.

[13] Rovida A, Locati M, Camassi R, Lolli B, Gasperini P (2019):Catalogo Parametrico dei Terremoti Italiani (CPTI15), versione 2.0. Istituto Nazionale di Geofisica e Vulcanologia (INGV). .

[14] Rossetto T, Elnashai A (2003): Derivation of vulnerability functions for European-type RC structures based on observational data.*Engineering Structures*. **25** , 1241–1263.

[15] Bianchini M (2008):Improved scalar intensity measures in performance-based earthquake engineering. .

[16] MATLAB (2019):R2019a Update 4(9.6.0.1150989). The MathWorks, Inc., Natick, Massachusetts.

[17] Boore DM, Watson-Lamprey J, Abrahamson NA (2006): Orientation-independent measures of ground motion.*Bulletin of the Seismological Society of America*. **96** (4 A), 1502–1511.

[18] Kaklamanos J, Baise LG, Boore DM (2011): Estimating unknown input parameters when implementing the NGA ground-motion prediction equations in engineering practice.*Earthquake Spectra*. **27** (4), 1219–1235.

[19] CEN (2004):Eurocode 8 : Design of structures for earthquake resistance —. .

[20] R Core Team (2019):R: A language and environment for statistical computing. Vienna, Austria.

[21] Baker JW, Luco N, Thompson EM, Worden CB, Wald DJ, Bradley BA (2018): Spatial and spectral interpolation of ground-motion intensity measure observations.*Bulletin of the Seismological Society of America*. **108** (2), 866–875.

[22] Jayaram N, Baker JW (2009): Correlation model for spatially distrributed ground-motion intensities.*Earthquake Engineering & Structural Dynamics*. **38** , 1678–1708.

[23] Bradley BA (2014): Site-specific and spatially-distributed ground-motion intensity estimation in the 2010-2011

Canterbury earthquakes.*Soil Dynamics and Earthquake Engineering*. **61**–**62** (2014), 83–91.

[24] Esposito S, Iervolino I (2011): PGA and PGV spatial correlation models based on European multievent datasets.*Bulletin of the Seismological Society of America*. **101** (5), 2532–2541.

[25] Goda K, Atkinson GM (2010): Intraevent spatial correlation of ground-motion parameters using SK-net data.*Bulletin of the Seismological Society of America*. **100** (6), 3055–3067.

[26] Dolce M, Papa F, Pizza AG (2002): Istruzione per la compilazione della scheda di 1° livello.

[27] Grünthal G (1998):European Macroseismic Scale 1998. in: Cah. Du Cent. Eur. Géodynamique Séismologie, Luxembourg.

